NETWORKS AND HETEROGENEOUS MEDIA
©American Institute of Mathematical Sciences
Volume **8**, Number **1**, March **2013**
doi:10.3934/nhm.2013.8.65
pp. **65–78**

GROWTH REGULATION AND THE INSULIN SIGNALING PATHWAY

Peter W. Bates and Yu Liang

Department of Mathematics
Michigan State University
East Lansing, MI 48824, USA

Alexander W. Shingleton

Department of Zoology
Michigan State University
East Lansing, MI 48824, USA

Abstract. The insulin signaling pathway propagates a signal from receptors in the cell membrane to the nucleus via numerous molecules some of which are transported through the cell in a partially stochastic way. These different molecular species interact and eventually regulate the activity of the transcription factor FOXO, which is partly responsible for inhibiting the growth of organs. It is postulated that FOXO partially governs the plasticity of organ growth with respect to insulin signalling, thereby preserving the full function of essential organs at the expense of growth of less crucial ones during starvation conditions. We present a mathematical model of this reacting and directionally-diffusing network of molecules and examine the predictions resulting from simulations.

1. **Dedication.** Hiroshi Matano has been an inpiration to the first author for more than three decades, opening his eyes to mathematical, cultural, and natural beauty. PWB takes this opportunity to express his gratitude on the occasion of Hiroshi Matano's sixtieth birthday. While this paper, describing a complex diffusive system, does not contain new fundamental mathematical principles as in most of the work of Hiroshi Matano, it has been influenced by his ability to see mathematics in all areas of life.

2010 *Mathematics Subject Classification.* Primary: 92-08, 92C42, 92C40; Secondary: 92C37, 92C30.

Key words and phrases. Cellular regulatory network, signaling pathway, nonlinear system of partial differential equations.

The first author is funded in part by NSF DMS 0908348, 0531898, and NIH 5 R01 GM090208-03.

The second author is funded in part by Cooperative Agreement No. DBI-0939454.

The third author is funded in part by the National Science Foundation under Grant No. IOS-0845847 and Cooperative Agreement No. DBI-0939454.

The first and second authors completed this work while visiting IMA and are pleased to acknowledge their support.

2. **Introduction.** The insulin and insulin-like signaling (IIS) pathway propagates a signal from receptors in the cell membrane to the nucleus via numerous molecules. Some of these molecules reside on or contiguous to the cell membrane, some reside in or contiguous to the nucleus and some are in the cytosol, being transported between these two regions in a somewhat stochastic way. Included in this pathway is the forkhead transcription factor FOXO, which promotes the expression of negative growth regulators ([10]). FOXO is negatively regulated by the insulin signaling pathway, and it is the reduction in insulin signaling and the resulting activation of FOXO that is, in part, responsible for inhibiting organ growth in conditions of reduced nutrition ([2]). The result is that organ growth is nutritionally plastic. However, different organs show different levels of nutritional plasticity, essential to ensuring that certain key organs, for example the mammalian brain, are largely spared the effects of malnutrition. Recent research has suggested that these differences in nutritional plasticity are mediated by differences in the structure of the insulin-signaling pathway in different organs. However, how changes in the structure of the insulin signaling pathway affects how the pathway regulates growth with respect to nutrition is unclear. Here we use mathematical modeling to help solve this problem.

Our starting point is a mathematical model of metabolic insulin signaling pathways devised by Sedaghat, Sherman, and Quon [9], in which a system of ordinary differential equations is presented describing the dynamical behavior of components of the insulin signaling pathway downstream of the insulin ligand. Although many of the protein components of the insulin signaling pathway are attached to, or associated with, the cell membrane they are all at some point transported through the cytoplasm. All proteins are synthesized at the endoplasmic reticulum (ER), which is contiguous with the nuclear membrane. The proteins are then packaged into vesicles, first by the ER and then by the Golgi apparatus, before these vesicle, and the proteins within them, are transported to their final destination. Vesicle transport is through the action of molecular motors, e.g. kinesin, which attach to the vesicle and walk it along the microtubules that form the cytoskeleton of the cell. Because the transportation process has a stochastic aspect to it, due to the distribution of motors and micro- tubules (or other scaffolding) and the processivity of the motors, this is modeled as an enhanced or directional diffusive process. For simplicity we use a spherically symmetric cell with the nuclear shell having radius r_1 and the cell membrane having radius r_2 ($r_1 < r_2$).

Among other things, this diffusive transport builds a delay into the dynamics described in [9], which may be important in regulation. We also include degradation and basal transcription of molecules into the model. As mentioned above, the growth of organs is negativly regulated in part by the transcription factor FOXO, the active state of which resides in the nucleus. A protein kinase, Akt, downstream from the insulin receptors, in its active (phosphorylated) state, deactivates FOXO by phosphorylating it. Phosphorylation of FOXO by Akt both inhibits its activity as a transcription factor and causes it to be transported out of the nucleus. The inactive FOXO in the cytoplasm can be reactivated and targeted for nuclear localization through phosphorylation or monoubiquitination by proteins in other signaling pathways. Importantly, activated FOXO promotes the transcription of the insuin receptor, creating a negative feedback loop between the top and the bottom of the pathway ([5]). Thus, our system becomes more complex by adding both molecular species with transcriptional feedback, and spatial transport of some

molecules. Part of our purpose for this is to determine the mechanism whereby organ size plasticity is regulated. We believe that this regulation of plasticity is achieved through the insulin-signaling pathway in general and FOXO specifically. Our model explores that hypothesis.

3. **The model.** We divide the system into several coupled subsystems, starting with the

3.1. **Insulin receptors subsystem.** Let I denote the concentration of insulin, which is a constant in this paper (we take two values of I when computing sensitivity). An insulin receptor in the cell membrane may bind one or two insulin molecules and when bound, autophosphorylation occurs and so initiates a signal transduction cascade. Receptors may also reside temporarily in the cytosol, where they are transported to the cell membrane.

Thus we have the state variables:

Receptors:

$R_1(t)$, concentration of unbound unphosphorylated cell-surface receptors,
$R_2(t)$, concentration of once-bound unphosphorylated cell-surface receptors,
$R_3(t)$, concentration of phosphorylated twice-bound cell-surface receptors,
$R_4(t)$, concentration of phosphorylated once-bound cell-surface receptors,
$R_5(r,t)$, concentration of unbound unphosphorylated intracellular receptors,
$R_6(r,t)$, concentration of phosphorylated twice-bound intracellular receptors,
$R_7(r,t)$, concentration of phosphorylated once-bound intracellular receptors.

PTP:

$P(r,t)$: A prefactor representing the relative activity of PTPases (the class of enzymes that regulate tyrosine kinase activity by removing a phosphate) in the cell. This factor depends upon the level of activated Akt, which varies according to a partial differential equation coupled to the rest of the system.

FOXO:

$F(r,t)$, concentration of activated FOXO,
$f(r,t)$, concentration of deactivated FOXO.

The synthesis of R_1: Free insulin receptors (R_1) on the membrane bind to insulin (I) and become once-bound unphosphorylated surface receptors (R_2) at the rate k_1. That reaction is reversible with rate k_{-1}. Phosphorylated once-bound surface receptors (R_4) are dephosphorylated by PTPases, release their insulin and become unbound unphosphorylated surface receptors (R_1) with rate $k_{-3}P$. At the same time, free surface receptors (R_1) pass through the cell membrane to become intracellular receptors (R_5) with rate k_4 and the intracellular receptors attach to the cell membrane, becoming surface receptors with rate k_{-4} ([6],[7]). Finally, a certain fraction (d) of receptors degrades and is lost. Therefore, the synthesis rate of free receptor on the membrane, R_1, is expressed by

$$\dot{R_1} = -k_1 I R_1 + k_{-1} R_2 + k_{-3} P R_4 + k_{-4} R_5(r_2, t) - k_4 R_1 - d R_1. \tag{1}$$

The synthesis of R_2: In addition to the exchanges with R_1, described above, the once-bound unphosphorylated surface receptors (R_2) degrade at the same rate d and are phosphorylated to become phosphorylated once-bound surface receptors

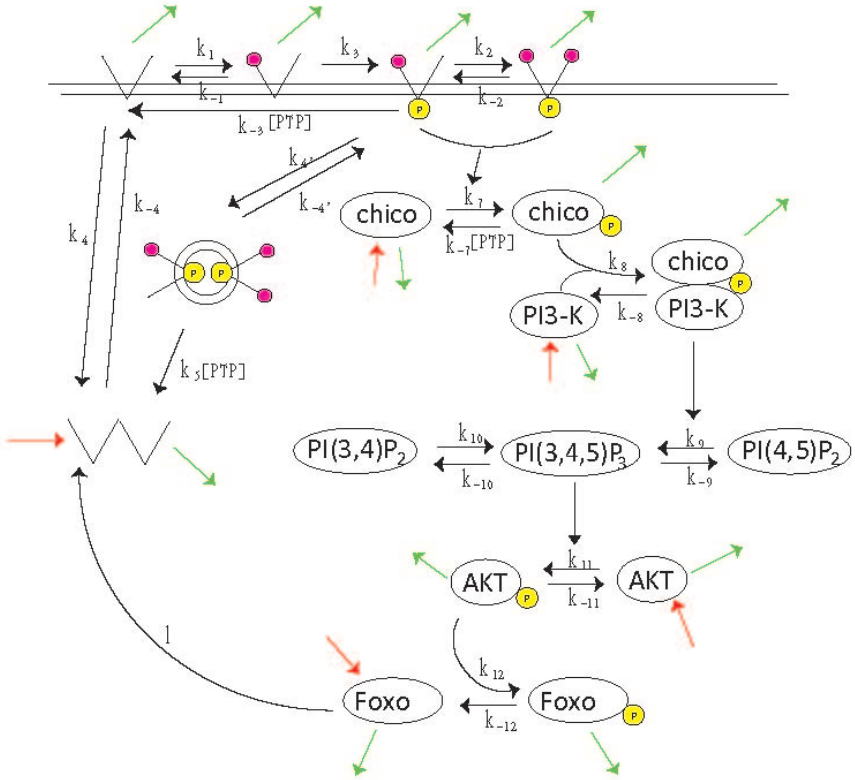

FIGURE 1. The Signalling Pathway

(R_4) at the rate k_3. Therefore, the synthesis rate of R_2 is

$$\dot{R_2} = k_1 I R_1 - k_{-1} R_2 - k_3 R_2 - d R_2. \tag{2}$$

The synthesis of R_3: Phosphorylated once-bound surface receptors (R_4) bind to insulin (I) and become phosphorylated twice-bound surface receptors (R_3) with rate k_2. This reaction is reversible with rate k_{-2}. At the same time, phosphorylated twice-bound surface receptors (R_3) pass through the cell membrane with rate $k_{4'}$ to become phosphorylated twice-bound intracellular receptors (R_6). This process is reversible with rate $k_{-4'}$. Therefore, the synthesis rate of R_3 is

$$\dot{R_3} = k_2 I R_4 - k_{-2} R_3 + k_{-4'} R_6(r_2, t) - k_{4'} R_3 - d R_3. \tag{3}$$

The synthesis of R_4: In addition to the exchanges with R_1, R_2, and R_3, described above, phosphorylated once-bound surface receptors (R_4) pass though the membrane with rate $k_{4'}$, becoming phosphorylated once-bound intracellular receptors (R_7). That process is reversible with rate $k_{-4'}$. Therefore, the synthesis rate of R_4 is

$$\dot{R_4} = -k_2 I R_4 - k_{-3} P R_4 + k_3 R_2 + k_{-2} R_3 + k_{-4'} R_7(r_2, t) - k_{4'} R_4 - d R_4. \tag{4}$$

The synthesis of R_5: The gene responsible for creating insulin receptors is transcribed in the nucleus and the resulting RNA passes through pores in the nuclear shell entering the cytoplasm. Once in the cytoplasm, with the help of a ribosome, translation starts to the protein (receptor) and is completed in the ER (endoplasmic reticulum), which is contiguous to the nucleus. The receptor is then packaged into vesicles (the vesicle membrane holds the receptor which is a transmembrane protein) and is taken to the Golgi apparatus, and then finally the cellular surface membrane. All via transport vesicles that are moved by one of the motor proteins along microtubules. Here, we simplify this process by postulating the production of free insulin receptors (R_5) on the nuclear surface ($r = r_1$) due in part to the activated transcription factor FOXO which enhances basal transcription. The resulting receptors are actively transported to the outer cell membrance, but in a stochastic way. Thus, R_5 has a spatio-temporal distribution that is governed by an equation with advection and diffusion terms, as well as reaction terms, exchanging between other states, and a degradation term. The advection-diffusion operator we employ has the form

$$Lu \equiv D\Delta u - \delta\nabla\cdot(\frac{\mathbf{x}}{|\mathbf{x}|}u),$$

giving radially-directed transport towards the cell membrane. In the equations below, we express this operator in radial coordinates since we assume spherical symmetry. Boundary conditions represent a FOXO-dependent source at r_1 and a sink at r_2, as receptors leave the cytoplasm to become embedded in the cell membrane. The way in which activated FOXO (F) operates in creating free receptors at the nucleus is modeled using the Michaelis-Menten relation, giving a term $l = \frac{\gamma\alpha F}{1+\alpha F}$, where α is a constant representing the affinity of FOXO binding to DNA and γ is a rate factor. We may also consider a mass-action reaction rate, which gives qualitatively similar results. The exchanges between other states in the cytoplasm include only intracellular receptors which are phosphorylated and have one or two insulin molecules bound become unphosphorylated at a rate k_6P, releasing their insulin, thereby contributing to R_5.

Therefore, the distribution of R_5 is described by

$$\frac{\partial R_5}{\partial t} = \frac{D}{r^2}\frac{\partial}{\partial r}(r^2\frac{\partial R_5}{\partial r}) - \frac{\delta}{r^2}\frac{\partial}{\partial r}(r^2R_5) - dR_5 + k_5P(R_6+R_7), \tag{5}$$

with boundary conditions obtained through a flux calculation,

$$D\frac{\partial R_5}{\partial r}(r_1,t) - \delta R_5(r_1,t) = -l - b_5, D\frac{\partial R_5}{\partial r}(r_2,t) - \delta R_5(r_2,t) = k_4R_1 - k_{-4}R_5,\ t>0.$$

The synthesis of R_6 and R_7: As described above, the twice-bound (R_6) and once-bound (R_7) intracellular receptors may pass through the membrane to become surface receptors, and vice-versa. Also these receptors become unphosphorylated at a rate k_6, releasing their insulin, and contributing to R_5. While in the cytosol, we assume that these receptors are actively transported towards the plasma membrane in the same way as the free receptos, that is, according to an advective and diffusive process. Again, their degradation rate is given by d. Therefore, the synthesis rates of R_6 and R_7 are

$$\frac{\partial R_6}{\partial t} = \frac{D}{r^2}\frac{\partial}{\partial r}(r^2\frac{\partial R_6}{\partial r}) - \frac{\delta}{r^2}\frac{\partial}{\partial r}(r^2R_6) - dR_6 - k_5PR_6, \tag{6}$$

with boundary conditions

$$D\frac{\partial R_6}{\partial r}(r_1,t)-\delta R_6(r_1,t)=0, \quad D\frac{\partial R_6}{\partial r}(r_2,t)-\delta R_6(r_2,t)=k_{4'}R_3-k_{-4'}R_6, \quad t>0,$$

and

$$\frac{\partial R_7}{\partial t}=\frac{D}{r^2}\frac{\partial}{\partial r}(r^2\frac{\partial R_7}{\partial r})-\frac{\delta}{r^2}\frac{\partial}{\partial r}(r^2R_7)-dR_7-k_5PR_7, \tag{7}$$

with boundary conditions

$$D\frac{\partial R_7}{\partial r}(r_1,t)-\delta R_7(r_1,t)=0, \quad D\frac{\partial R_7}{\partial r}(r_2,t)-\delta R_7(r_2,t)=k_{4'}R_4-k_{-4'}R_7, \quad t>0.$$

3.2. **Chico-PI3K complex subsystem.** Chico is an insulin receptor substrate, which acts as a scaffold bringing together other molecules responsible for the signal. PI3Ks are a family of related intracellular signal transducer enzymes capable of phosphorylating the 3 position of a lipid when in a complex with Chico. Phosphorylated insulin-bound surface receptors phosphorylate Chico, leading to the Chico-PI3K complex in the cell, a product upstream of the activation of Akt and the deactivation of FOXO.

In this subsystem, the state variables are Chico:
$C_1(r,t)$, concentration of unphosphorylated Chico,
$C_2(t)$, concentration of phosphorylated Chico,
and PI3K:
$\Phi_3(r,t)$, concentration of deactivated PI3K,
$\Xi(t)$, concentration of phosphorylated Chico-PI3K complex.

The synthesis of C_1: As with free receptors, the gene for Chico is transcribed in the nucleus and the RNA is translated to unphosphorylated Chico at a location contiguous to the nuclear membrane from where it is actively transported to the cell membrane. At the cell membrane the phosphorylated surface receptors (R_3 and R_4) phosphorylate Chico according to a mass-action law with rate k_7. Also, phosphorylated Chico (C_2) is dephosphorylated by PTPases according to a mass-action reaction with rate k_{-7}. The basal transcription rate of unphosphorylated Chico is denoted by b_c and it degrades at a rate denoted by d_c. Therefore, the synthesis rate of unphosphorylated Chico is

$$\frac{\partial C_1}{\partial t}=\frac{D}{r^2}\frac{\partial}{\partial r}(r^2\frac{\partial C_1}{\partial r})-\frac{\delta}{r^2}\frac{\partial}{\partial r}(r^2C_1)-d_cC_1, \tag{8}$$

with boundary conditions

$$\begin{aligned}
&D\frac{\partial C_1}{\partial r}(r_1,t)-\delta C_1(r_1,t)=-b_c,\\
&D\frac{\partial C_1}{\partial r}(r_2,t)-\delta C_1(r_2,t)=k_{-7}PC_2-k_7C_1(R_3+R_4).
\end{aligned}$$

The synthesis of C_2: Phosphorylation of Chico by surface receptors (R_3 and R_4) is described above, as is its dephosphorylation by PTPases. Phosphorylated Chico (C_2) binds with deactivated PI3K (Φ_3) according to mass-action kinetics forming the Chico-PI3K complex (Ξ) at a rate denoted by k_8. The dissociation of the phosphorylated Chico-PI3K complex into its two components takes place at

a rate denoted by k_{-8}. Phosphorylated Chico degrades at a rate denoted by d_c. Therefore, the synthesis rate of phosphorylated Chico is

$$\dot{C}_2 = k_7 C_1(r_2,t)(R_3+R_4) + k_{-8}\Xi - k_{-7}PC_2 - k_8\Phi_3(r_2,t)C_2 - d_cC_2. \quad (9)$$

The synthesis of Φ_3: This unphosphorylated PI3 kinase is translated adjacent to the nucleus from where it is transported to the cell membrane, as with other proteins described above. The basal transcription rate of unphosphorylated PI3K is denoted by b_p and the degradation rate is denoted by d_p. As mentioned above the dissociation rate of the phosphorylated IRS-PI3K complex is denoted by k_{-8}. Therefore, the synthesis rate of unphosphorylated PI3K is

$$\frac{\partial\Phi_3}{\partial t} = \frac{D}{r^2}\frac{\partial}{\partial r}(r^2\frac{\partial\Phi_3}{\partial r}) - \frac{\delta}{r^2}\frac{\partial}{\partial r}(r^2\Phi_3) - d_p\Phi_3, \quad (10)$$

with boundary conditions

$$D\frac{\partial\Phi_3}{\partial r}(r_1,t) - \delta\Phi_3(r_1,t) = -b_p, \quad D\frac{\partial\Phi_3}{\partial r}(r_2,t) - \delta\Phi_3(r_2,t) = -k_8\Phi_3(r_2,t)C_2 + k_{-8}\Xi.$$

The synthesis of Ξ: As mentioned above, through a mass-action reaction the production rate of the phosphorylated Chico-PI3K complex is denoted by k_8 and the dissociation rate is denoted by k_{-8}. We use d_{pc} to denote the degradation rate of phosphorylated PI3K-Chico complex. Therefore, the synthesis rate of phosphorylated Chico-PI3K complex (Ξ) is

$$\dot{\Xi} = k_8C_2\Phi_3(r_2,t) - k_{-8}\Xi - d_{pc}\Xi. \quad (11)$$

3.3. **Lipids subsystem.** Adjacent to the cell membrane, the phosphorylated Chico-PI3K complex (Ξ) converts the substrate phosphatidylinositol 4,5-bisphosphate ($PI(4,5)P_2$) to the substrate product phosphatidylinositol 3,4,5-trisphosphate ($PI(3,4,5)P_3$). Furthermore, there is spontaneous phosphorylation and dephosphorylation giving transitions between these two states and between $PI(3,4,5)P_3$) and another, $PI(3,4)P_2$. Some of these are catalyzed by PTEN and SHIP, whose concentrations we take to be constant and are implicitly included in the rate constants shown below. We assume that the total amount of PIP is conserved.

Let
$P_3(t)$ be the concentration of $PI(3,4,5)P_3$,
$P_4(t)$ be the concentration of $PI(3,4)P_2$,
$P_5(t)$ be the concentration of $PI(4,5)P_2$.

Conservation gives $L \equiv P_3 + P_4 + P_5$ is constant.

The equations to describe the synthesis rates of P_3, P_4 and P_5 are

$$\dot{P}_3 = k_{9p}\Xi P_5 + k_{9b}P_5 + k_{10}P_4 - k_{-9}P_3 - k_{-10}P_3, \quad (12)$$

$$\dot{P}_4 = k_{-10}P_3 - k_{10}P_4, \quad (13)$$

$$\dot{P}_5 = k_{-9}P_3 - (k_{9p}\Xi + k_{9b})P_5. \quad (14)$$

3.4. **Akt subsystem.** Akt is also known as Protein Kinase B (PKB), and as this name suggests it is a (serine/threonine) protein kinase, that is, it acts as a catalyst for protein interactions. It is produced in the vicinity of the nucleus, in its inactive or unphosphorylated state from where it is actively transported to the cell membrane where it becomes phosphorylated by the lipid $PI(3,4,5)P_3$.

The state variables for Akt are denoted by:
$A(r,t)$, concentration of deactivated Akt,
$A_p(r,t)$, concentration of activated Akt.

The synthesis of A and A_p: The basal transcription to unphosphorylated Akt (A) is denoted by b_A and its degradation rate (decay constant) is denoted by d_A. We assume that the degradation of activated Akt (A_p) occurs at the same rate. The lipid $PI(3,4,5)P_3$ (P_3) phosphorylates inactive Akt at a rate proportional to the concentrations of this lipid and of A with the rate constant denoted by k_{11}. Activated Akt is dephosphorylated spontaneously and becomes deactivated Akt with the rate k_{-11}. Also, activated Akt is transported from the cell membrane to the nucleus, where it interacts with activated FOXO, deactivating it through phosphorylation ([13]). Hence, the equations to describe the synthesis rates of A and A_p are

$$\frac{\partial A}{\partial t} = \frac{D}{r^2}\frac{\partial}{\partial r}(r^2\frac{\partial A}{\partial r}) - \frac{\delta}{r^2}\frac{\partial}{\partial r}(r^2 A) - d_A A + k_{-11}A_p, \tag{15}$$

with boundary conditions

$$D\frac{\partial A}{\partial r}(r_1,t) - \delta A(r_1,t) = -b_A, \quad D\frac{\partial A}{\partial r}(r_2,t) - \delta A(r_2,t) = -k_{11}A(r_2,t)P_3,$$

and

$$\frac{\partial A_p}{\partial t} = \frac{D}{r^2}\frac{\partial}{\partial r}(r^2\frac{\partial A_p}{\partial r}) + \frac{\delta}{r^2}\frac{\partial}{\partial r}(r^2 A_p) - d_A A_p - k_{-11}A_p, \tag{16}$$

with boundary conditions

$$D\frac{\partial A_p}{\partial r}(r_1,t) + \delta A_p(r_1,t) = 0, \quad D\frac{\partial A_p}{\partial r}(r_2,t) + \delta A_p(r_2,t) = k_{11}A(r_2,t)P_3.$$

3.5. **FOXO subsystem.** As indicated above, FOXO is a transcription factor, coding for insulin receptors among other proteins. Its active state is unphosphorylated but activated Akt phosphorylates FOXO, making it inactive ([3]). In its inactive state, FOXO leaves the nucleus and, while in the cytoplasm, spontaneously becomes unphosphorylated, and is transported back to the nucleus ([11]). We assume that both states of FOXO degrade in the cytoplasm at a common rate d_f (see [4]) and that active FOXO has a basal transcription rate of b_F in the nucleus.

The state variable for FOXO are denoted by:
$F(r,t)$, concentration of activated FOXO,
$f(r,t)$, concentration of deactivated FOXO.

To model the process of Akt phosphorylating FOXO at the nuclear membrane, we notice that when activated Akt interacts with activated FOXO, a small amount of temporary complex $[AF]$ forms quickly. Then $[AF]$ degrades to free activated Akt and phosphorylated FOXO f.

Using the Michaelis-Menten formalism, assuming quasi steady state for this fast reaction, and ignoring higher order terms of small quantities, we find the production

of phosphorylated FOXO f is proportional to the amount of [AF]:

$$k_{12}\frac{\beta A_p F}{(\beta+1)F+A_p},$$

where β is the ratio of the rate at which the $[AF]$ forms to the rate at which it dissociates.

We thus have the synthesis rates of F and f:

$$\frac{\partial F}{\partial t}=\frac{D}{r^2}\frac{\partial}{\partial r}(r^2\frac{\partial F}{\partial r})+\frac{\delta}{r^2}\frac{\partial}{\partial r}(r^2F)+k_{-12}f-d_fF, \tag{17}$$

with boundary condition

$$D\frac{\partial F}{\partial r}(r_1,t)+\delta F(r_1,t)=k_{12}\frac{\beta A_p F(r_1,t)}{(\beta+1)F(r_1,t)+A_p(r_1,t)}-b_F,$$

$$D\frac{\partial F}{\partial r}(r_2,t)+\delta F(r_2,t)=0,$$

and

$$\frac{\partial f}{\partial t}=\frac{D}{r^2}\frac{\partial}{\partial r}(r^2\frac{\partial f}{\partial r})-\frac{\delta}{r^2}\frac{\partial}{\partial r}(r^2f)-k_{-12}f-d_ff, \tag{18}$$

with boundary condition

$$D\frac{\partial f}{\partial r}(r_1,t)-\delta f(r_1,t)=-k_{12}\frac{\beta A_p F(r_1,t)}{(\beta+1)F(r_1,t)+A_p(r_1,t)},$$

$$D\frac{\partial f}{\partial r}(r_2,t)-\delta f(r_2,t)=0.$$

3.6. **PTPases.** In the model in [9], the activity of PTPases, P, is described as a piecewise linear function of the percentage of activated Akt (the ratio of activated Akt over total Akt) in such a way that P degenerates to zero when the percentage of activated Akt exceeds 36.4%, in accordance with experimental data. To get smoothness of $P(r,t)$, we use an exponential function instead to model the activity of PTPases:

$$P(r,t)=e^{-kA_p(r,t)}, \tag{19}$$

where the coefficient k is chosen by fitting to the piecewise linear function above.

4. **The results.** It is possible to show that the large system of reaction-diffusion equations coupled to ODE's through boundary values has a unique solution, existing for all time, at least for nonnegative initial data. However, the point of interest here is the qualitative behavior of solutions, and in particular, whether or not the system reproduces experimental data. We will also be interested in the evolution of the pathway and to what extent it is robust and optimized in some sense. These will be topics of further study. The results we report here are twofold:

I. Insulin signalling leads to a reduction in activated FOXO

The insulin (or more generally, insulin-like) signalling pathway regulates the growth of the cell through the negative growth regulator, FOXO. Specifically, developmental nutrition leads to the release of insulin-like peptides in the blood stream. When insulin is high, FOXO is phosphorylated downstream along the IIS pathway. This disrupts DNA binding and causes FOXO to translocate to the cytoplasm. A decline in insulin leads to an accumulation of active FOXO in the nucleus, increasing

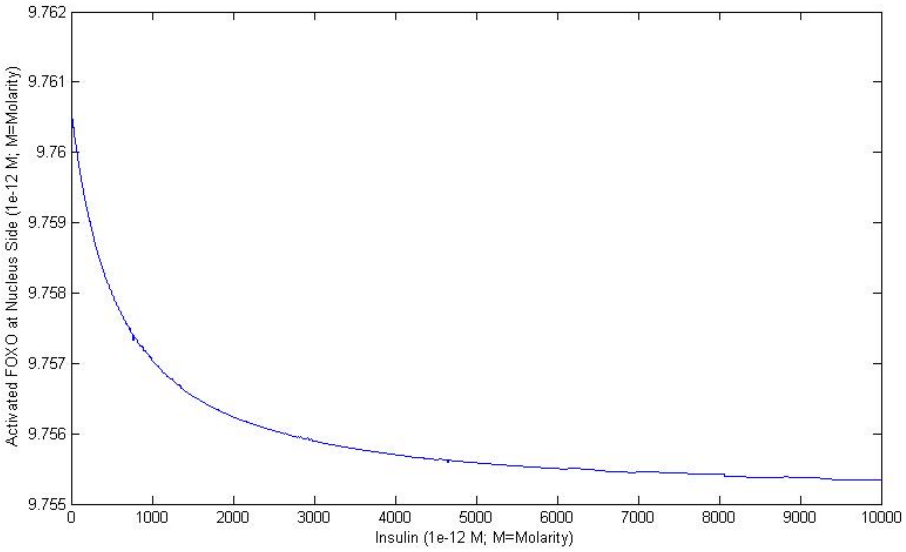

FIGURE 2. Nuclear FOXO vs. Insulin

the transcription of growth inhibitors. Also, the transcription of insulin receptors increases, which strengthens the insulin signal and thus moderates the increase of growth inhibitors. In the figure 2, we vary the concentration of model input–insulin and look at the concentration of activated FOXO in the nucleus at 10 minutes ($F(r_1, 10)$). The concentration of activated FOXO decreases as the concentration of insulin increases. This agrees with our understanding of the IIS pathway.

II. The sensitivity of activated FOXO is regulated by the expression of total FOXO

For animals, all the organs of an individual share the same structure of IIS pathway. However, not all organs show the same growth response to changes in developmental nutrition. For instance, in the fruit fly, *Drosophila melanogaster*, a reduction in developmental nutrition has more of an effect on wing size than on genital size, and this is a consequence of genital growth being less sensitive to changes in IIS. Similarly, in mammals the developing brain is relatively insensitive to changes in nutrition, a phenomenon called head sparing. Such organ-specific differences in nutritional- and insulin-sensitivity is fundamental to ensure that final body proportion is correct across a range of adult sizes.

Work on *Drosophila* has revealed that the reduced insulin-sensitivity of the genitalia is a consequence of changes in the expression of key genes in the IIS pathway, specifically the forkhead transcription factor FOXO ([12]). In order to verify the hypothesis with our model, we define the Sensitivity of Activated FOXO as the differences of the concentration of activated FOXO in the nucleus ($F(r_1, 10)$) at two insulin levels:

$$\text{Sensitivity} = F(r_1, 10; I_1) - F(r_1, 10; I_2)$$

where the two insulin levels are $I_1 = 1$ picomol and $I_2 = 10^5$ picomol.

Then by fixing the degradation rate of activated FOXO and manipulating the basal transcription rate, we change the expression of FOXO. Consequently, the sensitivity of activated FOXO is a function of the basal transcription rate. In Figure 3, the simulation shows that the sensitivity of activated FOXO increases as the basal transcription rate increases from 0 to 10 picomolar/min. Thus the sensitivity of activated FOXO to the signal from the IIS pathway is manipulated by the expression of FOXO itself, which verifies our hypothesis.

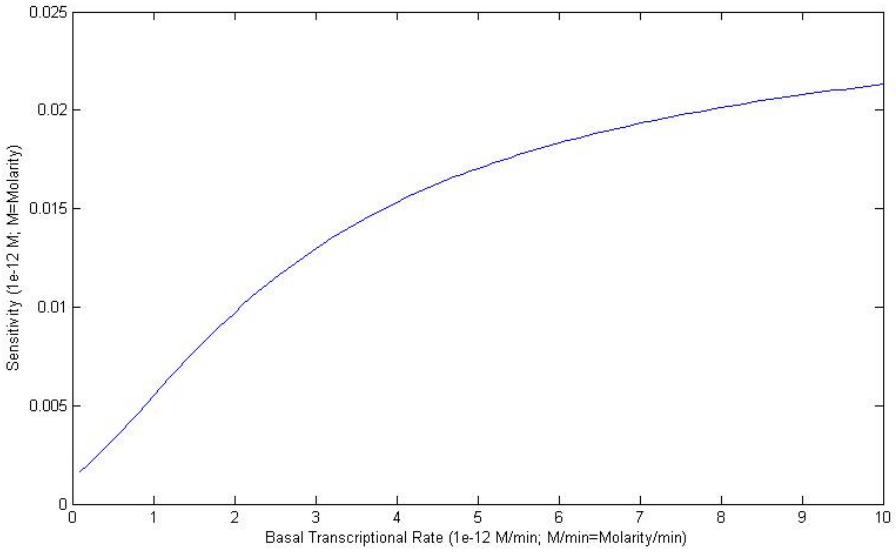

FIGURE 3. The Sensitivity of Activated FOXO

Appendix.

Variables and parameters in the model. In the tables below, pM = picomolar and μm = micrometer.

The prefactor k in the exponent of (19) was taken to be 0.03 based on the observation that activated Akt inhibits the action of PTP1B with a 25% decrease after maximal insulin stimulation. The ratio of activated Akt to deactivated Akt is 1:10 after the maximal insulin simulation ([9]) and the total steady state amount of Akt is taken to be 100 pM, and so from (19) k should be $0.11 * \log \frac{4}{3}$. The radius of cell, r_2, was chosen to be 6 μm based on experimental data that gives the cross-sectional area of *Drosophila* wing cells ranging from 87.59 μm^2 to 279.83 μm^2 ([8]). Assuming the radius of a cell nucleus is half that of the cell, which is common, we took r_1 to be 3 μm. We performed simulations with other values of r_1 and r_2 giving very similar results. In ([1]), transport by molecular motors is given as being around 800 $nm \cdot sec^{-1}$ which is about 50 $\mu m \cdot min^{-1}$. Thus, we took δ to be 50. We took D to be 25, equivalent to assuming that 5% of the molecules are transported by diffusion. The rate of feedback, γ, from activated FOXO to insulin receptors is unknown and we took it to be unity. Other unknown parameters, taken to be unity for lack of experimatal data, include α, the affinity coefficient of the activated FOXO

Model variables:

$R_1(t)$	concentration of unbound unphosphorylated cell-surface receptors
$R_2(t)$	concentration of once-bound unphosphorylated cell-surface receptors
$R_3(t)$	concentration of phosphorylated twice-bound cell-surface receptors
$R_4(t)$	concentration of phosphorylated once-bound cell-surface receptors
$R_5(r,t)$	concentration of unbound unphosphorylated intracellular receptors
$R_6(r,t)$	concentration of phosphorylated twice-bound intracellular receptors
$R_7(r,t)$	concentration of phosphorylated once-bound intracellular receptors
$P(r,t)$	A prefactor representing the relative activity of PTPases
$C_1(r,t)$	concentration of unphosphorylated Chico
$C_2(t)$	concentration of phosphorylated Chico
$\Phi_3(r,t)$	concentration of deactivated PI3K
$\Xi(t)$	concentration of phosphorylated Chico-PI3K complex
$P_3(t)$	concentration of $PI(3,4,5)P_3$
$P_4(t)$	concentration of $PI(3,4)P_2$
$P_5(t)$	concentration of $PI(4,5)P_2$
$A(r,t)$	concentration of deactivated Akt
$A_p(r,t)$	concentration of activated Akt
$F(r,t)$	concentration of activated FOXO
$f(r,t)$	concentration of deactivated FOXO

Parameters from [9]:

Parameters	Unit
$k_1 = 6 \times 10^{-5}$	$pM^{-1} \cdot min^{-1}$
$k_{-1} = 0.2$	min^{-1}
$k_2 = k_1$	min^{-1}
$k_{-2} = 20$	min^{-1}
$k_3 = 2500$	min^{-1}
$k_{-3} = 0.2$	min^{-1}
$k_4 = 0.0003$	min^{-1}
$k_{-4} = 0.003$	min^{-1}
$k_{4'} = 2.1 \times 10^{-3}$	min^{-1}
$k_{-4'} = 2.1 \times 10^{-4}$	min^{-1}
$k_6 = 0.461$	min^{-1}
$k_7 = 4.638$	min^{-1}
$k_{-7} = 1.396$	min^{-1}
$k_8 = 0.707$	$pM^{-1} \cdot min^{-1}$
$k_{-8} = 10$	min^{-1}
$k_{-9} = 42.148$	min^{-1}
$k_{9b} = 0.131$	min^{-1}
$k_{9p} = 1.390$	min^{-1}
$k_{10} = 2.961$	min^{-1}
$k_{-10} = 2.77$	min^{-1}
$k_{11} = 2.484$	min^{-1}
$k_{-11} = 6.932$	min^{-1}

binding with the DNA, β, the affinity coefficient for activated Akt binding with

New parameters:

Parameters	Unit
$k = 0.03$	1
$k_{12} = 1$	$pM^{-1} \cdot min^{-1}$
$k_{-12} = 1$	min^{-1}
$\alpha = 1$	1
$\beta = 1$	1
$\gamma = 1$	pM
$r_1 = 3$	μm
$r_2 = 6$	μm
$D = 25$	$\mu m^2 \cdot min^{-1}$
$\delta = 50$	$\mu m \cdot min^{-1}$
$d = 0.1$	min^{-1}
$d_c = 0.1$	min^{-1}
$d_p = 0.1$	min^{-1}
$d_{pc} = 0.1$	min^{-1}
$d_A = 0.1$	min^{-1}
$d_f = 0.1$	min^{-1}
$b_5 = 5$	$pM \cdot min^{-1}$
$b_c = 5$	$pM \cdot min^{-1}$
$b_p = 5$	$pM \cdot min^{-1}$
$b_A = 5$	$pM \cdot min^{-1}$

activated FOXO, k_{12}, the other parameter in the Michaelis-Menten reaction deactivating FOXO, and k_{-12} the rate at which deactivated FOXO is dephosphorylated in the cytoplasm, thus returning to its active state. The degradation coefficients are assumed to be 0.1 min^{-1} and the basal transcripiton constants ranging from 0 to 10 $pM \cdot min^{-1}$ were based on the initial conditions of the molecular concentrations in the original ODE model ([9]).

Simulation of the model. The simulation of the PDE-ODE system of 18 equations, was performed using the MATLAB solver–pdepe. The ODEs are treated by converting them to parabolic equations with large diffusivity. We obtain computationally stable solutions with $\Delta t = 0.01$ and $\Delta r = 0.1$.

REFERENCES

[1] Robert P. Erickson, Zhiyuan Jia, Steven P. Gross and Clare C. Yu, *How molecular motors are arranged on a cargo is important for vesicular transport*, PLoS Comput Biol., **7** (2011), 1–22.

[2] Ahmed Essaghir, Nicolas Dif, Catherine Y. Marbehant, Paul J. Coffer and Jean-Baptiste Demoulin, *The transcription of FOXO genes is stimulated by FOXO3 and repressed by growth factors*, J. Biol. Chem., **284** (2009), 10334–10342.

[3] Geert J. Kops, Nancy D. de Ruiter, Alida M. Vries-Smits, David R. Powell, Johannes L. Bos and Boudewijn M. Burgering, *Direct control of the Forkhead transcription factor AFX by protein kinase B*, Nature, **398** (1999), 630–634.

[4] Hitomi Matsuzaki, Hiroaki Daitoku, Mitsutoki Hatta, Keiji Tanaka and Akiyoshi Fukamizu, *Insulin- induced phosphorylation of FKHR (Foxo1) targets to proteasomal degradation*, Proc. Natl. Acad. Sci. U S A, **100** (2003), 11285–11290.

[5] Oscar Puig and Robert Tjian, *Transcriptional feedback control of insulin receptor by dFOXO/FOXO1*, Genes & Dev., **19** (2005), 2435–2446.

[6] Michael J. Quon and L. A. Campfield, *A mathematical model and computer simulation study of insulin receptor regulation*, J. Theor. Biol., **150** (1991), 59–72.
[7] Michael J. Quon and L. A. Campfield, *A mathematical model and computer simulation study of insulin-sensitive glucose transporter regulation*, J. Theor. Biol., **150** (1991), 93–107.
[8] Jaime Resino and Antonio García-Bellido, *Drosophila genetic variants that change cell size and rate of proliferation affect cell communication and hence patterning*, Mechanisms of Development, **121** (2004), 351–364.
[9] Ahmad R. Sedaghat, Arthur Sherman and Michael J. Quon, *A mathematical model of metabolic insulin signaling pathways*, Am. J. Physiol. Endocrinol. Metab., **283** (2002), 84–101.
[10] Alexander W. Shingleton, *The regulation of organ size in drosophila*, Organogenesis, **6** (2010), 1–13.
[11] Graham R. Smith and Daryl P. Shanley, *Modelling the response of FOXO transcription factor to multiple post-translational modifications made by ageing-related signalling pathways*, PLoS ONE, **5** (2010), 1–18.
[12] Huiyuan Tang, Martha S. B. Smith-Caldas, Michael V. Driscoll, Samy Salhadar and Alexander W. Shingleton, *FOXO regulates organ-specific phenotypic plasticity in drosophila*, PLoS Genet., **7** (2011), 1–12.
[13] Lars P. Van Der Heide, Marco F. M. Hoekman and Marten P. Smidt, *The ins and outs of FoxO shuttling: Mechanism of FoxO translocation and transcriptional regulation*, Biochem. J., **380** (2004), 297–309.

Received April 2012; revised January 2013.

E-mail address: bates@math.msu.edu
E-mail address: liangyu2@msu.edu
E-mail address: shingle9@msu.edu